

Support Information for

Degradation of phenol accumulated in a micellar molybdovanadophosphate nanoreactor by air at ambient temperature and atmospheric pressure

*Shun Zhao, Congliang Song, Lei Wang, Xiaobin Xu, Xiaohong Wang**

Key Lab of Polyoxometalate Science of Ministry of Education, Faculty of Chemistry
Northeast Normal University, Changchun 130024, P. R. China
Fax: (+86) 431-85099759
E-mail: wangxh665@nenu.edu.cn

General Information

All solvents and chemicals were used as obtained from commercial supplies. Centrifugation was performed on T4C Centrifuge (10000rpm, 5 min, Beijing Yiyao). Elemental analysis was carried out using a Leeman Plasma Spec (I) ICP-ES and a P-E 2400 CHN elemental analyzer. FTIR spectra ($4000\text{-}400\text{ cm}^{-1}$) were recorded in KBr discs on a Nicolet Magna 560 IR spectrometer. Dynamic light scattering (DLS) was employed in order to study the size of the reverse-micelles in the Microtrac S3500 Particle Analyzer in terms of the hydrodynamic radius. Analysis of phenol and intermediates during the reaction was performed by high pressure liquid chromatogram (HPLC, Shimadzu LC-20A) with a UV detector using a Shim-pack VP-ODS ($4.6\times 250\text{mm}$, $5\mu\text{m}$) column. The mobile phase was a mixture of 80% water, and 20% methanol with a flow rate of 1 mL/min. Total organic carbon (TOC) was monitored using a Shimadzu TOC-VCPH total organic carbon analysis system. COD in influent and effluent samples was determined by a closed reflux colorimetric method using 756 CRT UV-vis spectrophotometer at a wavelength of 600 nm. TEM image was recorded with JOEL JEM-2100F microscope. The leaching concentrations of the catalyst during the reaction were also measured through analyzing the dissolved concentration of Mo in aqueous solution using a Leeman Plasma Spec (I) ICP-ES. XPS were recorded on an Escalab-MK II photoelectronic spectrometer with Al K_{α} (1200 eV). The cyclic voltammograms were recorded with an CHI660c recorder (China).

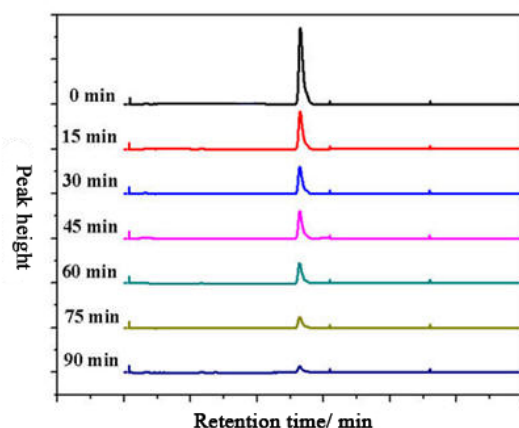


Figure S1. HPLC for the degradation of phenol by air.

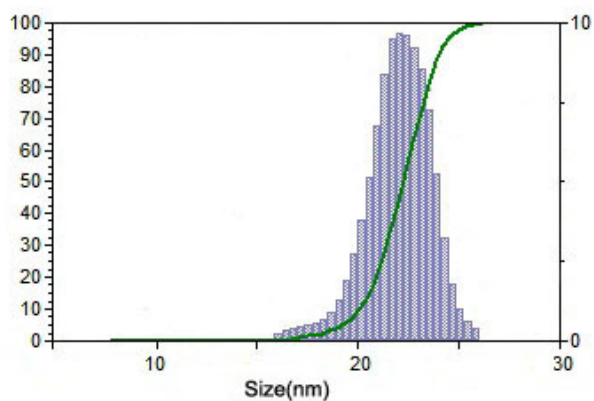


Figure S2. DLS pattern of $(C_{16}TA)_5PV_2Mo_{10}O_{40}$ in 0.1 mg mL^{-1} aqueous solution.

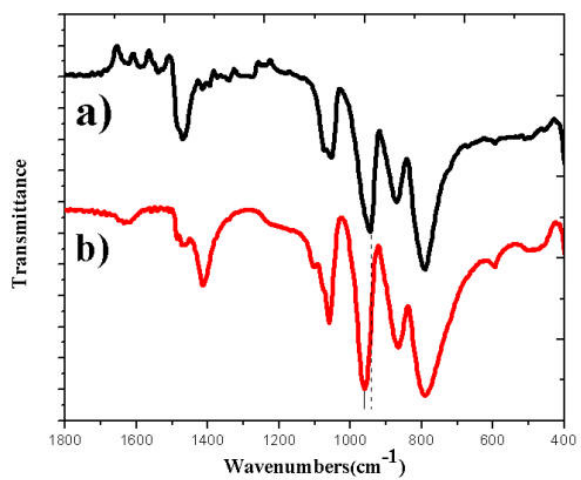


Figure S3. The IR spectra of $(C_{16}TA)_5PV_2Mo_{10}O_{40}$ (a) and $(C_{16}TA)_5PV_2Mo_{10}O_{40}$ adsorption of phenol (b).

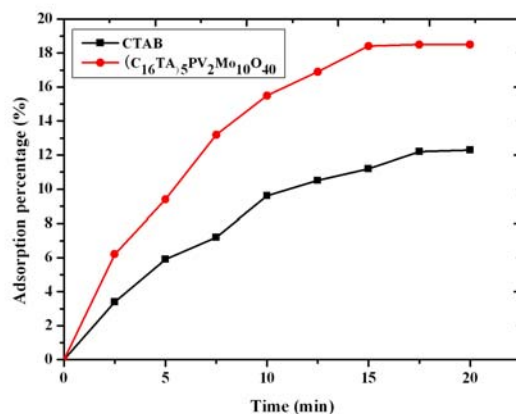


Figure S4. The adsorption percentages of phenol on $(C_{16}TA)_5PV_2Mo_{10}O_{40}$ and CTAB.

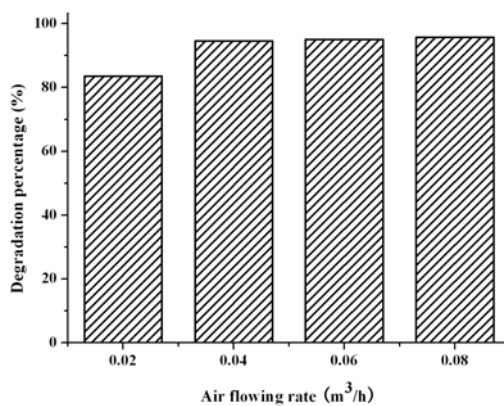


Figure S5. The influence of air flowing rate on phenol degradation (100 mL of 0.72 mM phenol solution) in the presence of $(C_{16}TA)_5PV_2Mo_{10}O_{40}$ (0.92 mM) at room temperature for 90 min.

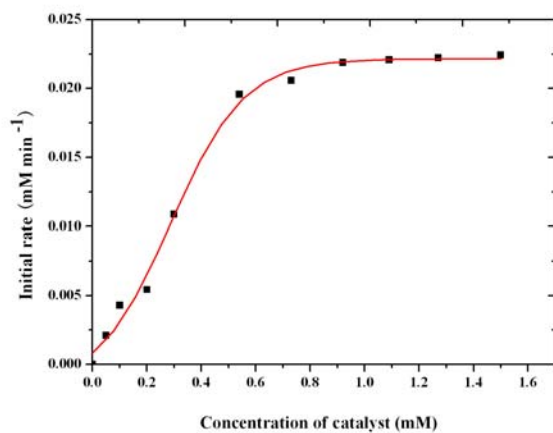


Figure S6. Initial rate vs. the concentration of catalyst $(C_{16}TA)_5PV_2Mo_{10}O_{40}$ in degradation of phenol in 100 mL of 0.72 mM phenol solution with the air flowing rate 0.04 m³/h at room temperature. The initial rate is based on the degradation after 15 min.

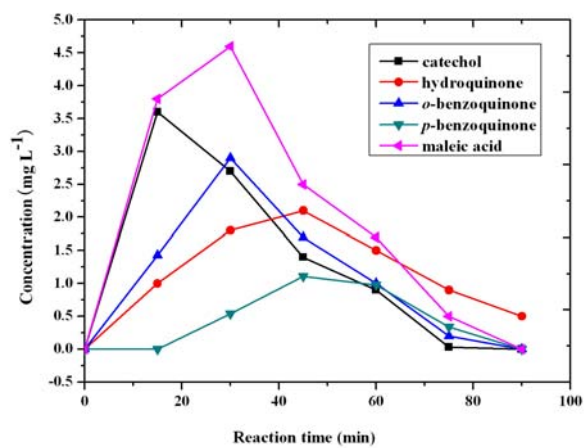


Figure S7. Evolution of hydroquinone, catechol, and then p-benzoquinone, o-benzoquinone, and maleic acid in the solution during CWAQ degradation of phenol with $(C_{16}TA)_5PV_2Mo_{10}O_{40}$ (0.92 mM) in 100 mL of 0.72 mM phenol solution with the air flowing rate 0.04 m³/h for 90min at room conditions.

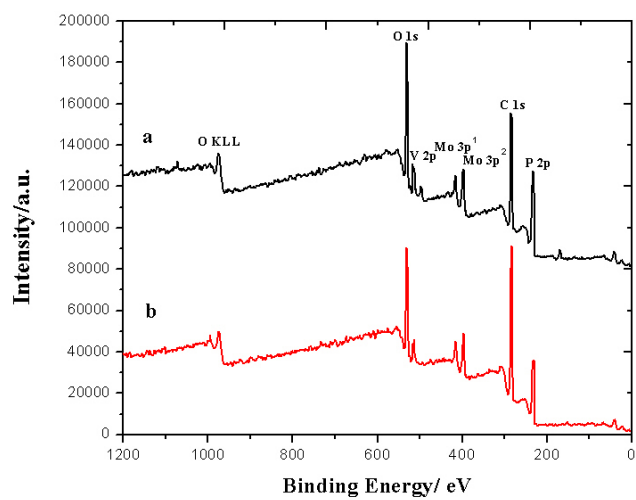


Figure S8. Survey XPS spectra of $(C_{16}TA)_5PV_2Mo_{10}O_{40}$ catalyst before (a) and after the reaction (b)